Cell. Mol. Life Sci. (2010) 67:629–640
DOI 10.1007/s00018-009-0200-6

Cellular and Molecular Life Sciences

RESEARCH ARTICLE

An isoform of the vacuolar (H^+)-ATPase accessory subunit Ac45

Eric J. R. Jansen · Nick H. M. van Bakel · Anthon J. M. Coenen · Sander H. van Dooren · Hermina A. M. van Lith · Gerard J. M. Martens

Received: 24 September 2009 / Revised: 20 October 2009 / Accepted: 2 November 2009 / Published online: 28 November 2009

Abstract The vacuolar (H^+)-ATPase (V-ATPase) is the main regulator of intraorganellar pH and in neuroendocrine cells is controlled by its accessory subunit, Ac45. Here, we report the discovery of the first isoform of a V-ATPase accessory subunit, namely an Ac45-like protein, denoted Ac45LP. Phylogenetic analysis revealed a lineage-dependent evolutionary history: Ac45 is absent in birds, and Ac45LP is absent in placental mammals, whereas all other tetrapod species contain both genes. In contrast to Ac45, Ac45LP is not proteolytically cleaved, a prerequisite for proper Ac45 routing. Intriguingly, *Xenopus* Ac45LP mRNA was expressed in developing neural tissue and in neural crest cells. In adult *Xenopus*, Ac45 mRNA is widely expressed mostly in neuroendocrine tissues, while Ac45LP mRNA expression was found to be restricted to the kidney and the lung. This novel Ac45LP may provide additional possibilities for V-ATPase regulation during neurodevelopment as well as in kidney and lung cells.

Keywords Ac45 isoform · ATP6AP1 · *Xenopus* · Development · Phylogenetic analysis · V-(H^+)-ATPase

Electronic supplementary material The online version of this article (doi:10.1007/s00018-009-0200-6) contains supplementary material, which is available to authorized users.

E. J. R. Jansen · N. H. M. van Bakel · A. J. M. Coenen · S. H. van Dooren · H. A. M. van Lith · G. J. M. Martens (✉)
Donders Institute for Brain, Cognition and Behaviour, and Nijmegen Centre for Molecular Life Sciences (NCMLS), Department of Molecular Animal Physiology, Radboud University Nijmegen, Geert Grooteplein Zuid 28, 6525 GA Nijmegen, The Netherlands
e-mail: g.martens@ncmls.ru.nl

Introduction

In eukaryotic cells, certain organelles, such as endosomes, lysosomes and secretory granules, must maintain an acidic internal environment in order to function properly. This intraorganellar acidification is mainly regulated by the vacuolar (H^+)-ATPase (V-ATPase), a large multi-protein complex which, at the expense of ATP, pumps protons from the cytosol into the lumen of the organelles. V-ATPase-mediated acidification has been extensively studied, and diverse critical processes have been identified to be dependent on this proton pump, including membrane trafficking, embryonic left–right patterning, receptor-mediated endocytosis, lysosomal hydrolysis, neurotransmitter release and prohormone processing [1–4]. In addition to its intraorganellar roles, V-ATPase is known to play an important role in extracellular acidification as well. In various specialized mammalian cells, such as the renal alpha-intercalated cells, the pump is located at the apical membrane where it regulates proton secretion into the late distal renal tubule in order to maintain an acid–base balance [5]. The V-ATPase in the apical membrane of osteoclasts is a major player in modulating bone resorption [6].

The V-ATPase also plays an essential role in the development of multicellular organisms. In the mouse, disruption of the V-ATPase complex by selective gene inactivation leads to early developmental lethality [7, 8]. In developing Drosophila, disruption of plasma membrane V-ATPase subunit alleles results in the lethal transparent Malpighian tubule phenotype, which is most likely the result of a failure in urinary acidification [9]. The treatment of *Xenopus* or chick embryos with the V-ATPase-specific inhibitor bafilomycin A1 resulted in a disturbance of embryonic left–right patterning [1], while a recent study on zebrafish V-ATPase mutants showed severe malformations

of the melanocytes and retinal pigmented epithelium of the developing eye [10]. Taken together, the results of these studies point to an important, conserved and broad role for V-ATPase proton pumping in developing organisms.

The V-ATPase consists of two main sectors. The cytoplasmic ATP-hydrolytic V1-sector is composed of subunits A, B, C, D, E, F, G and H. The membranous V0-sector consists of subunits a, e, d, c and c″ and harbors the rotary mechanism that is used to transport protons across the membrane [11]. Intriguingly, extensive expression studies on V-ATPase subunits in tissues of various species have identified the existence of a number of isoforms of V-ATPase subunits throughout the animal kingdom. V-ATPase subunit isoforms expressed predominantly in the kidney have been reported for the V0a4 subunit with a repertoire of splice variants [12–14], for the V1B1 subunit [15] and, more recently, for the V0d2, V1G3 and V1C2 subunits [5, 16, 17]. In neurons, three V0a isoforms are expressed (V0a1-3), whereas alternative splicing of V0a1 mRNA results in brain-specific variations of this subunit [18]. In *Caenorhabditis elegans*, four distinct V0a isoforms have been identified [19]. Furthermore, a repertoire of V-ATPase subunit isoforms has been discovered in the apical pole of narrow and clear cells of the epididymis where they regulate the pH to keep spermatozoa in a quiescent state during their maturation and storage [20]. Expression of the V-ATPase subunit isoform V1C2a has also been found, specifically in the lamellar bodies of type II alveolar lung cells, whereas its relative V1C2b is expressed uniquely in the α- and ß- kidney intercalated cells [21]. Clearly, the diversity of V-ATPase subunit isoforms and thus the numerous subunit combinations provide cells with highly specialized proton pumps, each situated in a specific membrane and with a distinct regulation.

In addition to the 'common' subunits and their isoforms, certain cell types possess an accessory subunit that binds to the V0-sector as part of the V-ATPase complex. The highly glycosylated type-I transmembrane protein Ac45 (ATP6AP1) is a neuroendocrine-enriched accessory subunit of the V-ATPase that was first isolated from bovine chromaffin granules by its co-purification with the V0-sector of the pump [22–24]. In secretory granules [22, 23] and in the ruffled apical membrane of osteoclasts [6, 25], the Ac45 protein binds to the V0-sector of the V-ATPase. In peptide-hormone-producing *Xenopus* melanotrope cells, the Ac45 protein is co-expressed with the main melanotrope secretory cargo protein, proopiomelanocortin (POMC), suggesting a role for Ac45 in V-ATPase-mediated acidification of the secretory pathway. We have therefore proposed that the Ac45 protein may be a regulatory subunit of the V-ATPase [26]. This hypothesis was recently supported by the results of our transgenic approach in the neuroendocrine *Xenopus* melanotrope cells, showing that Ac45 controls V-ATPase localization by directing the V-ATPase into the regulated secretory pathway, thereby affecting V-ATPase-mediated and Ca^{2+}-dependent regulated secretion [27].

In contrast to what holds for the 'common' V-ATPase subunits, no isoform of the V-ATPase accessory subunits has been found. In the study reported here, we describe and characterize for the first time a relative of the Ac45 protein. On the basis of our results, we propose that this newly identified, lung- and kidney-specific Ac45 isoform may influence V-ATPase functioning during development and in adult organisms in a tissue-specific manner.

Materials and methods

Databases and phylogenetic and protein structure prediction analysis

Expressed sequence tag (EST) and genomic sequences were derived from NCBI using the TBlastN algorithm (http://www.ncbi.nlm.nih.gov/) and from the Ensembl genome browser (http://www.ensembl.org/index.html) and UCSC genome browser (http://genome.ucsc.edu/) using the BLAST algorithm. Multiple alignments of EST sequences were performed by ContigExpress (Vector NTI Suite 7 software package). Nucleotide sequences were translated using the ExPASy-Translate tool (http://www.expasy.ch/tools/dna.html). Alignments were made using ClustalW (http://www.ebi.ac.uk/Tools/clustalw2/index.html) and edited in JalView 2.3 [28]. Phylogenetic trees were calculated using the PHYLIP 3.68 package (http://evolution.gs.washington.edu/phylip.html) and plotted with TreeDyn [29]. An overview of search references is listed in Electronic Supplementary Material (ESM) Table S1. The public CBS Prediction Server (http://www.cbs.dtu.dk/services/) was used to predict protein domains and post-translational modifications.

Animals

Female *Xenopus laevis* were obtained from African Reptile Park (Muizenberg, South Africa) and reared under day–night conditions at 18°C in the *Xenopus* facility of the Department of Molecular Animal Physiology, Central Animal Facility, Radboud University, Nijmegen, The Netherlands. Experiments were carried out in accordance with the European Communities Council Directive 86/609/EEC for animal welfare.

Xenopus eggs and embryos

Eighteen hours prior to obtaining the eggs, female *X. laevis* were injected with 375 iU human chorionic gonadotropin

(Pregnyl; Organon, Oss, The Netherlands). For in vitro fertilization, eggs were harvested and directly put in contact with sperm of a freshly dissected testis. After 5 min, the eggs were overlaid with 0.1× MMR (1× MMR; 100 mM NaCl, 2 mM KCl, 1 mM $MgCl_2$, 1.5 mM $CaCl_2$, 5 mM Hepes, pH 7.5). The fertilized eggs were then selected and cultured in 0.1× MMR/50 µg/ml gentamycin at 22°C. Various developmental embryonic stages were selected and used for total RNA extractions. Embryo staging was carried out according to Nieuwkoop and Faber [30].

Molecular cloning of *Xenopus laevis* Ac45LP cDNA

For molecular cloning of the full-length nucleotide sequence of *Xenopus* Ac45LP, cDNA derived from total RNA isolated from stage-25 *Xenopus* embryos was used as a template. For PCR amplification, High Fidelity PCR Enzyme Mix (Fermentas Int, Burlington, ON, Canada) with primers based on *Xenopus* embryonic EST sequences (accession no. BJ036521, xAc45LP forward primer: 5′-gggggtacctcgagccttttgcaaat**atg**ctggcttc-3′; accession no. AW766525, xAc45LP reverse primer: 5′-gggggagctc tagatcaatcccacaggttg**tta**ttctg -3′) was used. After amplification, the PCR products were subcloned into the pGEM-T-Easy Vector System (Invitrogen, Carlsbad, CA), and inserts were sequenced on both strands using T7 and SP6 sequencing primers and various internal primers using the ABI BigDye Sequencing kit (Applied Biosystems, Foster City, CA). The *Xenopus* Ac45LP cDNA sequence was deposited in the NCBI GenBank under accession no. GQ427149.

For exogenous protein expression in *Xenopus* embryos, both full-length *Xenopus* Ac45 (clone X1311) [24, 26] and Ac45LP cDNAs were subcloned into the $pCS2^+$ vector for in vitro transcription using SP6-RNA polymerase.

In vitro transcription and microinjection of synthetic mRNAs into *Xenopus* embryos

Ac45/$pCS2^+$ and Ac45LP/$pCS2^+$ plasmids were linearized with *Not*I, and 1 µg of linearized DNA was used as a template for in vitro transcription using the Message Machine SP6 Transcription kit (Ambion, Foster City, CA) according to the manufacturer's guidelines. Following synthesis, the mRNA was precipitated using lithium chloride and dissolved in DEPC-treated MQ. The jelly-coat was removed from in vitro fertilized *Xenopus* eggs using 2% cysteine in 0.25× MMR (1× MMR; 100 mM NaCl, 1 mM KCl, 0.5 mM $MgCl_2$, 1.5 mM $CaCl_2$, 5 mM Hepes, pH 8.2), and the fertilized eggs were subsequently washed in 0.1× MBS [1× MBS; 88 mM NaCl, 0.82 mM $MgSO_4$, 2.4 mM $NaHCO_3$, 1 mM KCl, 0.33 mM $Ca(NO_3)_2$, 0.41 mM $CaCl_2$, 10 mM Hepes, pH 7.4], placed in an injection grid filled with injection medium (3% Ficoll/ 0.25× MMR/50 µg/ml gentamycin) and kept on a cooled plate. Following the injection of RNA [1–2 ng mRNA/ 10 nl MR solution (100 mM NaCl, 1.8 mM KCl, 2 mM Ca Cl_2, 1 mM $MgCl_2$, 5 mM Hepes, pH 7.6] into the animal hemisphere, embryos were allowed to recover for 2 h and initiate first embryonic cleavages at 18°C. Well-developing four-cell stage embryos were selected and cultured in injection medium at 18°C until developmental stage 12 was reached, at which point ten embryos were homogenized in 100 µl lysis buffer [50 mM Hepes pH 7.4, 140 mM NaCl, 0.1% Triton-X100, 1% Tween 20, 1 mg/ml deoxycholate, 1 µM phenylmethylsulfonyl fluoride (PMSF), 0.1 mg/ml soybean trypsin inhibitor]. The lysates were cleared by centrifugation, and 5 µl of the supernatant was subjected to western blot analysis.

Western blot analysis

Embryo lysates were separated on 10% SDS–PAGE and subsequently transferred to nitrocellulose membrane (Protran; Schleicher and Schuell, Dassel, Germany). Membranes were incubated with the anti-Ac45-C antibody (1311-C, 1:5,000) [24] and secondary peroxidase-conjugated Goat-anti-Rabbit antibody (Nordic Immunology, Tilburg, The Netherlands, 1:5,000) followed by chemoluminescence (LumiLight ^{Plus}; Roche Diagnostics, Indianapolis, IN). Signals were detected using a Bio-Imaging system with Labworks 4.0 software (UVP BioImaging systems, Cambridge, UK).

Digoxigenin-UTP labeling of *Xenopus* Ac45 and Ac45LP RNA probes

For the generation of *Xenopus* Ac45 and Ac45LP sense- and anti-sense digoxigenin (DIG)-labeled RNA probes, we amplified a 304-bp fragment of *Xenopus* Ac45 cDNA (clone X1311 nt 401–704) [24]) by PCR using the primers x1311-5′ISH(5′-ggg**gaattc**gagaagcttggagtcagc) and x1311-3′ISH(5′-ggg**gaattc**taggctgctcagtggcaag). For the amplification of a 306-bp *Xenopus* Ac45LP cDNA fragment (this manuscript, GenBank accession no. GQ427149, nt 377-682), we used primers xAc45LP-5′ISH (5′-ggg**gaattc**aaaaccaggcaaactggaac) and xAc45LP-3′ISH (5′-ggg**gaattc**gtacagtggtatcaaggctc). After purification, the PCR products were bidirectionally cloned into the *Eco*RI-restriction site of pGEM3-Zf+ (Promega Life Sciences, Madison, WI). The orientation of the inserts was verified by DNA sequencing using the T7-promoter primer. Both sense- and anti-sense-oriented clones of the Ac45 and Ac45LP inserts were selected. A 1-µg aliquot of *Bam*HI-linearized plasmid DNA was used for the synthesis of

DIG-labeled RNA probes using the DIG-RNA Labeling Mix (Roche Diagnostics) and T7-RNA polymerase (Fermentas) according to the manufacturers' guidelines. After a lithium chloride precipitation, the purified RNA was dissolved in DEPC-treated MQ. For quantifying the amount of DIG-labeled RNA probe, we spotted a dilution series of the probe and of a reference dilution series of DIG-labeled control RNA (Roche Diagnostics) onto a nitrocellulose membrane (Stratalinker UV Crosslinker; Stratagene, San Diego, CA). The membrane was washed in TBS (136 mM NaCl, 2.7 mM KCl, 25 mM Tris, pH 7.4), incubated in blocking buffer (2% NGS, 1% BSA in TBS) for 30 min, incubated with anti-DIG–alkaline phosphatase-conjugated Fab fragments (1:5,000 in blocking buffer) for 1 h at 22°C, washed twice for 15 min with TBS and pre-incubated in alkaline phosphatase buffer (AP-buffer; 100 mM NaCl, 100 mM Tris pH 9.5). Finally, the blot was stained using NBT/BCIP substrate (Roche Diagnostics) in AP-buffer, and the concentrations of the DIG-labeled probes were determined.

Whole-mount in situ hybridization

Stage-30 *Xenopus* embryos were fixed in MEMFA (0.1 M MOPS, 2 mM EGTA, 1 mM $MgSO_4$, 4% parformaldehyde, pH 7.4), dehydrated in a graded series of ethanol and stored in 100% ethanol at −20°C. For in situ hybridization, embryos were rehydrated, incubated in TBS-T (1× TBS, 0.1% Tween-20), and Proteinase K treated (150 ng Proteinase K/ml in TBS-T) for 20 min at 50°C. The embryos were then washed for 10 min with 0.1 M triethanolamine/5 μl/ml acetic anhydride, twice with TBS-T and post-fixed in MEMFA for 20 min. After several washes with TBS-T, the embryos were incubated in pre-hybridization buffer (50% hybridization buffer, 50% TBS-T) for 10 min at room temperature (RT), placed in hybridization buffer [5× SSC pH 7.0, 50% formamide, 100 μg/ml Torula RNA, 0.1% Tween-20, 5 mM EDTA, 1.5% blocking reagent (Roche Diagnostics)] and pre-hybridized for 5 h at 58°C. The DIG-labeled RNA probes were then added (500 ng/ml), and hybridization was performed at 58°C for 16 h. The hybridization mix was then removed, and the embryos were washed three times with 2× SSC at 65°C for 20 min and treated for 30 min at 37°C with 5 μg/ml RNase A in 2× SSC. The embryos were subsequently washed with 0.2× SSSC (0.2× SSC, 0.3% CHAPS) for 20 min at 65°C, washed twice with MNT (100 mM maleic acid, pH 7.5, 150 mM NaCl, 0.1% Tween-20) at RT and pre-incubated in blocking buffer (1% Blocking Reagent in MNT) for 1 h. The embryos were then incubated with anti-DIG alkaline phosphatase-conjucated Fab fragments (Roche Diagnostics; 1:3,000 in blocking buffer) for 4 h at RT, rinsed several times with MNT and washed thoroughly with MNT at RT for 16 h. Finally, the embryos were washed with AP-buffer containing 2 mM levamisole (Roche Diagnostics) and stained using BM Purple AP substrate (Roche Diagnostics). Embryos were examined under a Leica MZ FLIII stereomicroscope and photographs were taken with a Leica DC200 color camera using the Leica DCviewer software.

Fig. 1 Phylogenetic analysis and alignment of Ac45 [accessory subunit of vacuolar (H^+)-ATPase] and Ac45-like protein (Ac45LP) sequences. **a** Sequence alignment. *Underlining* Transmembrane region, *asterisks* conserved cysteine residues. The alignment contains *colors* utilized by the ClustalX coloring algorithm in JalView (conservation grade colors and coloring of amino acid residues according to physicochemical criteria). **b** Phylogenetic tree: *Aa Aedes aegypti*, *Ac Anolis carolinensi*, *Bf Branchiostoma floridae*, *Ce Caenorhabditis elegans*, *Cf Canis familiaris*, *Dm Drosophila melanogaster*, *Dr Danio rerio*, *Ga Gasteroteus aculeatus*, *Gg Gallus gallus*, *Hs Homo sapiens*, *Tg Taeniopygia guttata*, *Md Monodelphis domestica*, *Mm Mus musculus*, *Oa Ornithorhynchus anatinus*, *Rn Rattus norvegicus*, *Xl Xenopus laevis*, *Xt Xenopus tropicalis* ▶

In situ hybridization of *Xenopus* embryo sections

Stage-30 *Xenopus* embryos were fixed in Bouin's fixative, dehydrated through a graded series of ethanol and embedded in paraffin. Sections (6 μm) were mounted on poly-L-lysine-coated slides and air dried for 16 h at 37°C. After deparaffination, sections were subsequently incubated with 0.1% pepsin/PBS (7 min), 2% paraformaldehyde (4 min) and 1% hydroxyl ammonium chloride/PBS (4 min). For in situ hybridization, sections were air dried and covered with 150 μl hybridization buffer (4× SSC, 50% formamide, 1× Denhardt's, 10% dextran sulfate, 25 mM sodium phosphate and 0.2 ng/ml yeast tRNA) containing a DIG-labeled RNA probe (100 ng/ml). Hybridization was performed at 55°C for 16 h in a humidified chamber. After washing with 2× SSC, 1× SSC, 0.5 × SSC at 20°C, sections were pre-incubated in blocking buffer (2% normal goat serum, 1% BSA, 0.3% Triton-X100 in TBS) for 30 min at 20°C and then incubated with anti-DIG alkaline phosphatase-conjucated Fab fragments (Roche Diagnostics, 1:500 in blocking buffer) for 2 h. After washing with TBS and AP-buffer, sections were stained using nitro-blue tetrazolium (Roche Diagnostics) and X-phosphate (Roche Diagnostics) in AP-buffer. Finally, sections were mounted in Mowiol and examined under a Leica DM 6000 B microscope.

Results

Identification and phylogenetic analysis of an Ac45 paralog

With the aim of identifying a structurally related relative of the Ac45 protein, we performed database searches and a

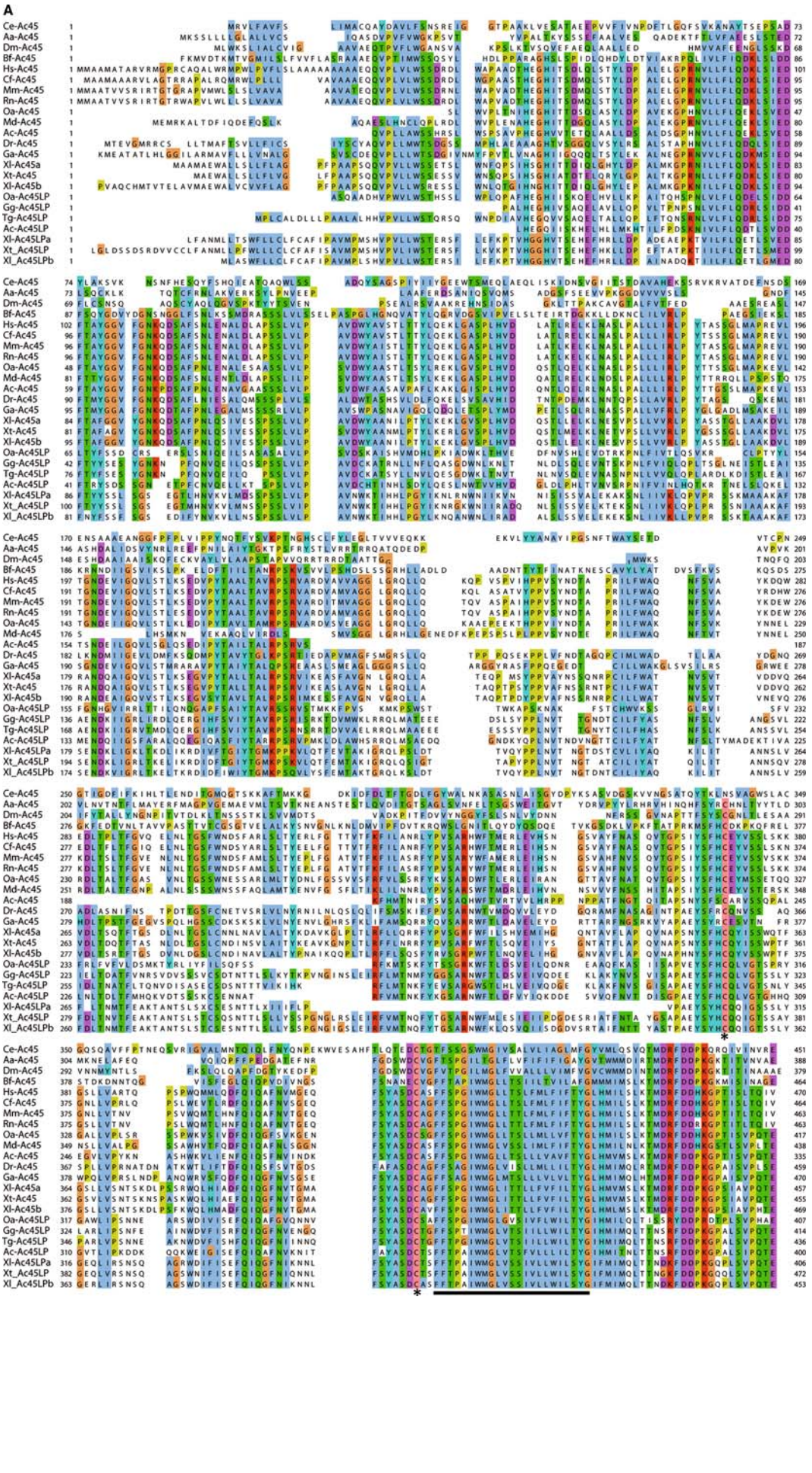
A
Ce-Ac45
Aa-Ac45
Dm-Ac45
Bf-Ac45
Hs-Ac45
Cf-Ac45
Mm-Ac45
Rn-Ac45
Oa-Ac45
Md-Ac45
Ac-Ac45
Dr-Ac45
Ga-Ac45
Xl-Ac45a
Xt-Ac45
Xl-Ac45b
Oa-Ac45LP
Gg-Ac45LP
Tg-Ac45LP
Ac-Ac45LP
Xl-Ac45LPa
Xt_Ac45LP
Xl_Ac45LPb

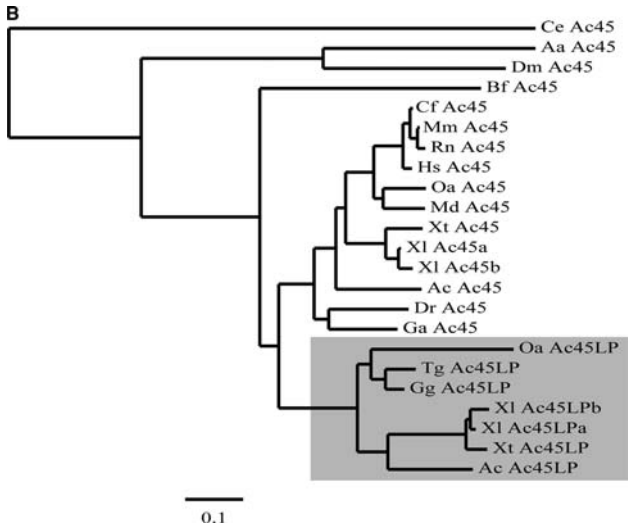

Fig. 1 continued

phylogenetic analysis using database sequences from a large variety of species: man (*Homo sapiens*), dog (*Canis familiaris*), rat (*Rattus norvegicus*), mouse (*Mus musculus*), opossum (*Monodelphis domestica*), Platypus (*Ornithorhynchus anatinus*), chicken (*Gallus gallus*), zebra finch (*Taeniopygia guttata*), lizard (*Anolis carolinensis*), frog (*Xenopus laevis* and *X. tropicalis*), zebrafish (*Danio rerio*), stickleback (*Gasteroteus aculeatus*), lancelet (*Branchiostoma floridae*), mosquito (*Aedes aegypti*), fly (*Drosophila melanogaster*) and worm (*Caenorhabditis elegans*). An overview of the identified genes is provided in ESM Table S1. To construct the phylogenetic tree, we used the ancestral Ac45 genes of *Drosophila*, *C. elegans*, *A. aegypti* and *B. floridae* as outgroups. Two separate branches were distinguished. The first branch contains the original Ac45 protein that has been found in vertebrates ranging from amphibians (*Xenopus*) and fish (*Danio rerio*) to mammals—but not in birds (*G. gallus* and *T. guttata*). The second branch harbors a group of Ac45-related proteins (Fig. 1a, b). As for Ac45, the primary structures of these newly identified Ac45 paralogs are characterized by the presence of two conserved cysteine residues and a highly homologous transmembrane domain. However, these Ac45-related proteins differ from Ac45 itself by the absence of the typical proline-rich region (amino acids 249–265 in human Ac45, Fig. 1a [31]) and a distinct C-tail. These characteristics led us to name this group Ac45-like proteins (Ac45LPs). Based on the results of our database searches and phylogenetic analysis, we identified Ac45LPs only in birds (*G. gallus* and *T. guttata*), frogs (*X. laevis* and *X. tropicalis*), lizard (*A. carolinensis*) and Platypus (*O. anatinus*), leading to the conclusion that the Ac45LP is found solely in tetrapods and not in placental mammals.

Loss of the Ac45LP gene in placental mammals

We studied the Ac45LP gene of the amphibian *X. tropicalis* as a representative of the tetrapod species. Browsing the translated *X. tropicalis* genomic database (Ensemble Genome Browser) with the *X. tropicalis* Ac45LP amino acid sequence as bait revealed, apart from the *X. tropicalis* Ac45 gene (ten exons) located on scaffold 1144, the Ac45LP gene situated at scaffolds 121 and 856 (ten exons).

To gain more insight into the evolutionary history of the Ac45LP gene, we studied the genomic sequences flanking the Ac45LP gene in human, mouse, chick, *Xenopus* and fish. In *Xenopus*, the surrounding genomic region of the Ac45LP gene consists of genes ASB15 and IQUB upstream of Ac45LP and genes SLC13A1 and FEZF1 downstream of Ac45LP. On chicken chromosome 1, the structural organizations of these genes, including that of the Ac45LP gene, were fully conserved (Fig. 2a). On human chromosome 6 and mouse chromosome 7, the locations of the Ac45LP-neighboring genes were also conserved; however, in the regions between the mammalian IQUB and SLC13A1 genes, we surprisingly identified only a partial sequence of exon 9 of the Ac45LP gene (Fig. 2a, b). In fish, the potential Ac45LP-surrounding genes were also fully conserved, but this species lacked any Ac45LP-related genomic sequences within this chromosomal fragment (Fig. 2a).

With respect to the Ac45 gene, in human, mouse, frog and fish we found complete conservation of its neighboring genes, RPL-10, TAZ (upstream), GDI1 and FAM50A (downstream). In contrast, we did not identify the Ac45 gene in chick and found the Ac45-neighboring genes to be scattered over a number of chromosomes (Fig. 2a). We conclude that in placental mammals the Ac45LP gene and in birds the Ac45 gene have been lost, and that in other tetrapods, both the Ac45 and the Ac45LP gene are still present (Fig. 2c).

Molecular cloning and characterization of Ac45LP in *Xenopus laevis*

To characterize the newly identified Ac45LP, we decided to clone the cDNA encoding the Ac45LP of *X. laevis*. To this end, we performed a BLAST search using the translated *Xenopus laevis* EST database (NCBI) and identified a number of 5′ and 3′ ESTs encoding partial protein sequences with a low degree of amino acid sequence identity to the N-terminal and C-terminal regions of the *Xenopus* Ac45 protein (31 and 39%, respectively). Based on these ESTs, we designed PCR primers and cloned a full-length *Xenopus* cDNA from a developmental stage-25 *X. laevis* cDNA pool. This cDNA contained a 1,359-bp open reading frame (ORF) encoding a protein of 453 amino

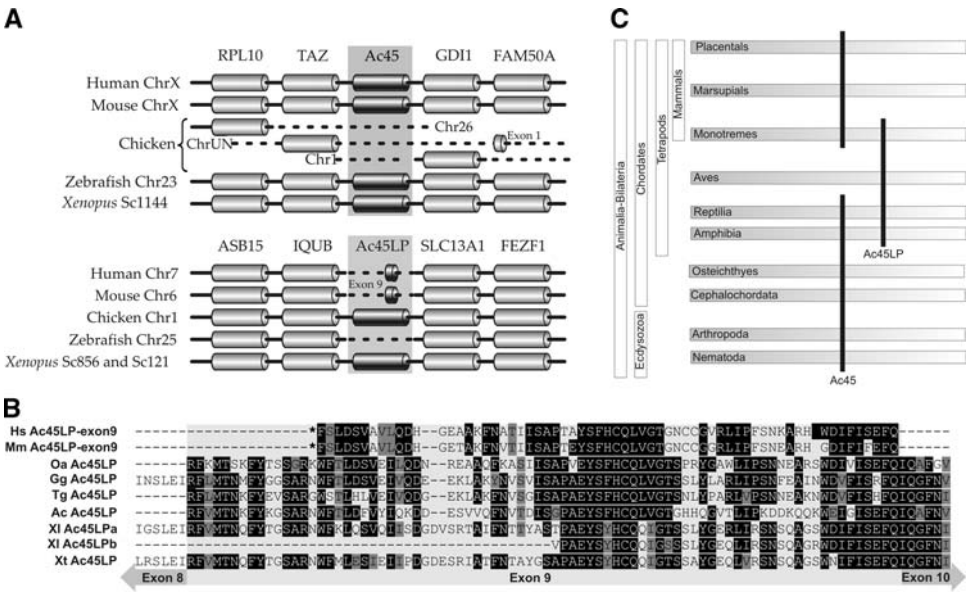

Fig. 2 The evolutionary history of the Ac45 and Ac45LP genes. **a** Schematic overview of genes surrounding the (presumptive) Ac45LP- and Ac45 genes. The Ac45LP gene was identified in chicken and *Xenopus*, but not in zebrafish. In human and mouse, only a remnant of the presumptive Ac45LP gene (*exon 9*) was found. The Ac45LP-neighboring genes were fully conserved. The Ac45 gene and its neighboring genes were fully conserved among species, with the exception of chicken. **b** Alignment of the partial human and mouse presumptive Ac45LP amino acid sequences (deduced from exon 9 Ac45LP sequences) with Ac45LP amino acid sequences from various species. *Asterisk* Stop codon preceding the exon 9 Ac45LP open reading frame. *Ac Anolis carolinensi*, *Gg Gallus gallus*, *Hs Homo sapiens*, *Tg Taeniopygia guttata*, *Mm Mus musculus*, *Oa Ornithorhynchus anatinus*, *Xl Xenopus laevis*, *Xt X. tropicalis*. **c** Lineage-dependent evolutionary fate of the Ac45 and Ac45LP genes

acids. The newly identified amino acid sequence showed 36.1% identity and 51.6% similarity with the *Xenopus* Ac45 protein sequence. Structure prediction programs (CBS Prediction Server) showed that the *Xenopus* Ac45LP amino acid sequence contains a potential signal peptide, eight potential *N*-glycosylation sites and a transmembrane region followed by a short cytoplasmic tail. Remarkably, the pairs of cysteines in the portion just N-terminal of the transmembrane region have also been conserved between *Xenopus* Ac45 and *Xenopus* Ac45LP (ESM Fig. S2).

Exogenous expression of Ac45 and Ac45LP in early *Xenopus* embryos

To study the biochemical properties of the Ac45LP, we performed exogenous protein expression studies in *Xenopus* embryos. To this end, one-cell stage *Xenopus* embryos were injected with synthetic Ac45 or Ac45LP mRNAs, and extracts of stage-12 embryos were subjected to western blot analysis. Since the epitope used for the generation of the anti-Ac45-C antibody (X1311-C [24]) is highly conserved between Ac45 and Ac45LP (ESM Fig. S2), this antibody was successfully applied to detect exogenous Ac45LP expression in the *Xenopus* embryos. The 62-kDa intact and glycosylated Ac45 protein as well as its cleaved and glycosylated 40-kDa form were observed in the lysates

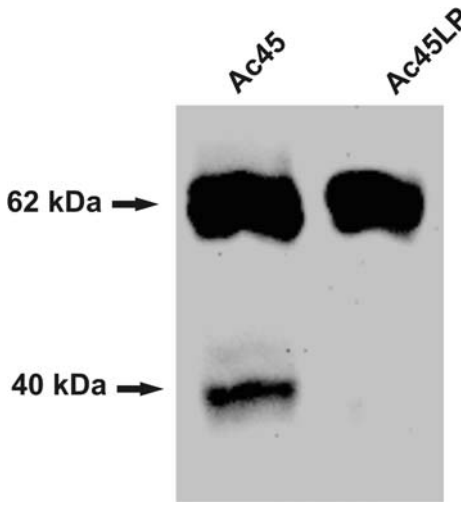

Fig. 3 Exogenous expression of Ac45 and Ac45LP in *Xenopus* embryos. Western blot analysis of lysates of embryos injected with synthetic Ac45 mRNA or Ac45LP mRNA. Ac45 and Ac45LP proteins were detected with an anti-Ac45-C antibody and visualized by chemoluminescence

of Ac45-mRNA-injected *Xenopus* embryos. In contrast, only the intact form of the Ac45LP, which migrated slightly slower than the 62-kDa intact Ac45 protein, was observed in the Ac45LP lysates (Fig. 3). Thus, *Xenopus* Ac45LP is not proteolytically cleaved.

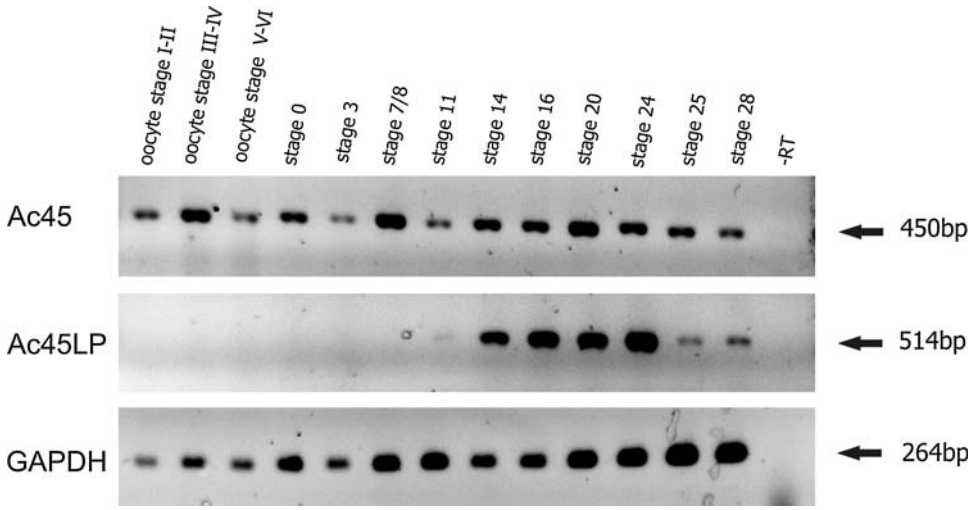

Fig. 4 Expression of Ac45 and Ac45LP mRNAs in developing *Xenopus*. Total RNA was extracted from *Xenopus* embryos (developmental stages are indicated). Reverse transcriptase-PCR analysis was performed as described in the Materials and Methods. Glyceraldehyde 3-phosphate dehydrogenase (*GAPDH*) served as an internal control for RNA integrity. *-RT* Absence of reverse transcriptase (negative control). Staging of *Xenopus* embryos was according to Nieuwkoop and Faber [30]

Analysis of Ac45 and Ac45LP mRNA expression during *Xenopus* development

A series of *Xenopus* developmental stages was analyzed for expression of Ac45 and Ac45LP mRNAs. Reverse transcriptase (RT)-PCR analysis showed that Ac45 mRNA was expressed in all maturing oocyte stages and in all of the developmental stages analyzed. In contrast, Ac45LP mRNA expression was found only from gastrulation stage (stage 11) onwards but decreased after stage 24 (Fig. 4). It would appear that Ac45 mRNA is both a maternal and an embryonic transcript, whereas Ac45LP mRNA is only embryonically expressed.

We then applied whole-mount in situ hybridization on stage-30 *Xenopus* embryos with an Ac45 as well as an Ac45LP DIG-labeled probe. Hybridization with the Ac45 anti-sense probe revealed clear hybridization signals in the developing brain and neural tube of the *Xenopus* embryos (Fig. 5a), whereas no signal was detected for the Ac45-sense probe (Fig. 5b). Using the Ac45LP anti-sense probe, however, we did not observe a hybridization signal (Fig. 5c). These results indicated that the whole-mount in situ hybridization technique was apparently not sensitive enough to detect Ac45LP mRNA expression. Taking into account that Ac45LP mRNA expression is presumably low and spatially restricted in *Xenopus* embryos, we then applied direct in situ hybridizations on *Xenopus* stage-30 embryonic sections. Using the Ac45 anti-sense probe, we found strong hybridization signals in the prosencephalon, mesencephalon and the developing eye (Fig. 6a, b), thereby supporting our whole-mount in situ hybridization data; Ac45 mRNA expression was also detected in neural crest cells distributed between the pharyngeal arches (Fig. 6b). No signals were detected for the Ac45-sense probe (Fig. 6c).

Only a low level of Ac45LP mRNA expression was detected in the developing brain (Fig. 6d) and eye (Fig. 6e), but when the direct hybridization approach was used, surprisingly clear signals were found in neural crest cells between the pharyngeal arches (Fig. 6e, f) and migrating through the ventral mesoderm (Fig. 6g). No hybridization signals were detected with the Ac45LP sense probe (Fig. 6h).

Thus, both Ac45 and Ac45LP mRNAs were expressed in *Xenopus* embryos, with the highest Ac45 mRNA expression levels in the developing brain, eye and neural crest cells; in contrast, the level of Ac45LP mRNA expression was relatively low in neural tissues but high in migrating neural crest cells.

Tissue distributions of Ac45 and Ac45LP mRNA in adult *Xenopus*

The mRNA distributions of Ac45 and Ac45LP were studied in tissues of adult *Xenopus*. In agreement with earlier studies on other species [22, 25, 26, 32], we found that Ac45 mRNA was ubiquitously expressed, with a higher abundance in the neuronal and neuroendocrine tissues of adult *Xenopus* (Fig. 7). Remarkably, and in contrast to Ac45, the expression of Ac45LP mRNA was restricted to the kidney and the lung of adult *Xenopus* (Fig. 7).

Discussion and conclusion

In the study reported here, we screened EST and genomic databases and identified the novel type I transmembrane protein Ac45LP that is related to the V-ATPase accessory subunit Ac45. To date, no isoform of a V-ATPase accessory subunit has been described. Our phylogenetic analysis

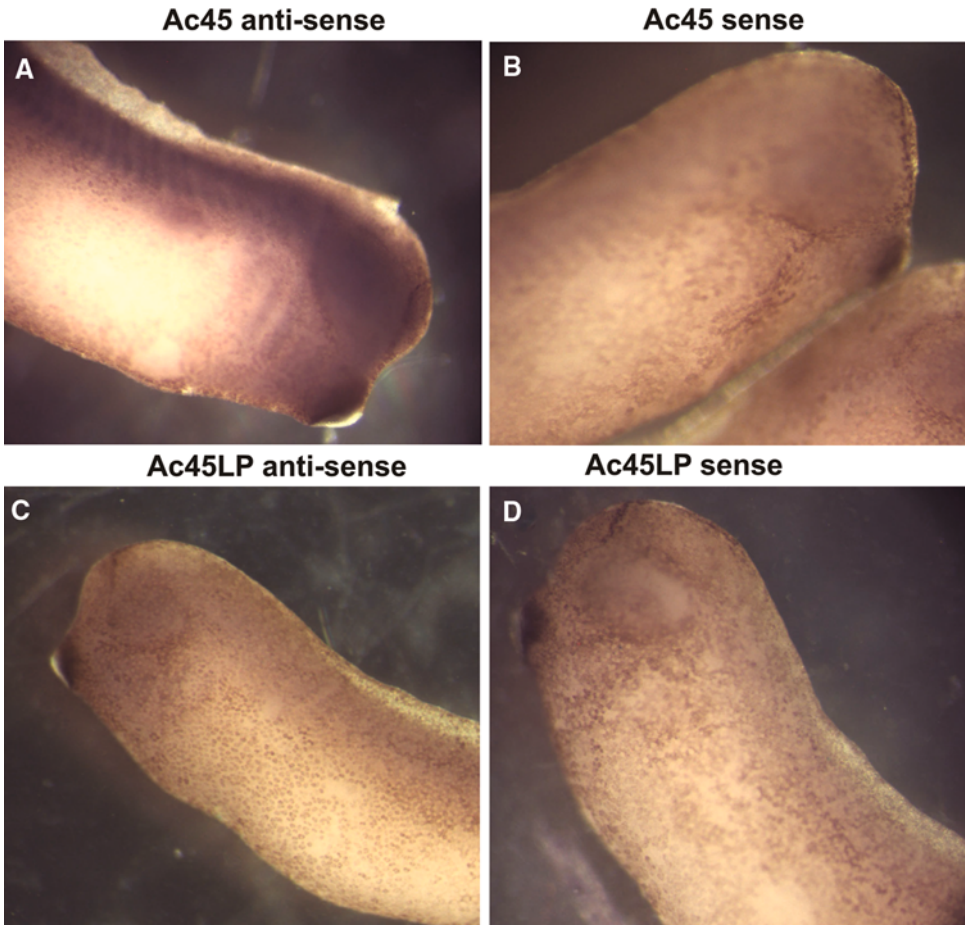

Fig. 5 Whole-mount in situ hybridization for Ac45 and Ac45LP mRNAs in stage-30 *Xenopus* embryos. Hybridizations with Ac45-anti-sense- (**a**) and Ac45-sense (**b**) DIG-labeled probes. Ac45 mRNA expression was predominantly found in developing neural tissues (brain, spinal cord and eye). **c** No signals were observed with the Ac45LP-anti-sense probe. **d** Negative control using the Ac45LP-sense probe

showed that the Ac45LP is highly conserved in tetrapod species, but that the gene was lost in placentals. This presumptive gene loss is supported by our identification of just a partial Ac45LP exon 9 sequence located in both human and mouse chromosomal regions syntenic to the Ac45LP genomic region in other tetrapods. Our search for Ac45LP sequences was successful in mammals only up to the Platypus, a Monotremata species. It would appear that during evolution, probably when the placentals and the marsupials diverged from the monotremes, the function of the Ac45LP was lost in the placental species, whereas the two regulators of the V-ATPase were sustained in other tetrapods. Intriguingly, the complete Ac45LP gene is present in birds, while our database searches did not identify any Ac45 gene fragments, leading us to conclude that the avian Ac45 gene has apparently been lost and that in birds Ac45LP acts as the only Ac45-related V-ATPase accessory subunit.

The overall structural characteristics of the Ac45LP clearly show similarities with those of the Ac45 protein; both polypeptides are highly glycosylated type I transmembrane proteins with conserved cysteine residues and a short C-tail. The Ac45 C-tail contains an autonomous targeting sequence, TMDRFDDPKG, that is highly conserved among species [31, 33]. Interestingly, this targeting signal is nearly identical to that in the Ac45LP (TNDKFDDPKG), and these signals may thus allow the co-existence of V-ATPases containing Ac45LP and V-ATPases containing Ac45 in the same membrane. On the other hand, the subtle variations in the targeting signals may direct Ac45LP to a cellular subcompartment distinct from that of Ac45, allowing each of the two proteins to execute a specific control of the V-ATPase.

The exogenous Ac45 protein was cleaved in developing *Xenopus* embryos injected with synthetic mRNAs, but the Ac45LP was not. Cleavage of the Ac45 protein has been shown to be a prerequisite for its transport through the secretory pathway of neuroendocrine *Xenopus* melanotrope cells [27]. Furthermore, a reduced proteolytic processing of Ac45 in furin $^{-/-}$ in pancreatic ß-cells is thought to be the cause of the impaired granular acidification found in these cells [32]. The fact that the Ac45LP sequence does not harbor a potential proprotein cleavage site is in line with our observation that Ac45LP is not cleaved in the injected *Xenopus* embryos. Ac45LP functioning does not seem to require its cleavage. It is

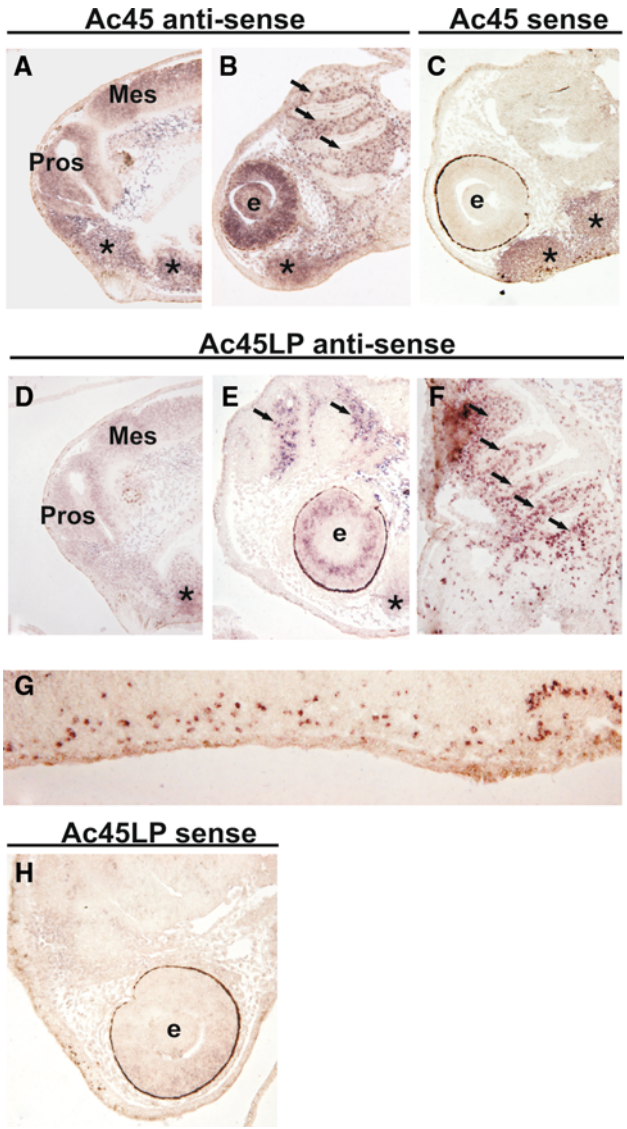

Fig. 6 Expression of Ac45 and Ac45LP mRNAs in neural tissue and neural crest cells of *Xenopus* embryos. Sections of developmental stage-30 *Xenopus* embryos hybridized with an Ac45-anti-sense probe showed Ac45 expression in the developing brain (**a**), in migrating neural crest cells between the pharyngeal arches and in the developing eye (**b**, *arrows*). No signals were detected with the Ac45-sense probe (**c**). Ac45LP mRNA expression was detected in the developing brain (**d**), in the migrating neural crest cells (**e**, **f**, *arrows*) and to a lower extent in the developing eye (**e**). Ac45LP mRNA-positive cells were also detected in the ventral mesoderm (**g**). No hybridization signal was found with the Ac45LP-sense probe (**h**). *Asterisk* Non-specific staining, *e* eye, *Pros* prosencephalon, *Mes* mesencephalon

possible that V-ATPases containing uncleaved Ac45LP and V-ATPases containing cleaved Ac45 are targeted to distinct subcompartments and/or contain different sets of subunit isoforms allowing differential functioning of the enzyme complex. However, we can not exclude the possibility that proteolytic processing of Ac45LP does occur in other cell types.

The presence of Ac45 mRNA in oocytes and in pre-gastrulation embryonic stages is interesting in that it points to a role for Ac45 in correct V-ATPase functioning during early developmental processes. V-ATPase-dependent proton fluxes have been shown to be critical for the regulation of correct left–right asymmetry in early embryos [1]. The absence of Ac45LP expression in these early developmental stages suggests that only Ac45—and not Ac45LP—is involved in proton pumping during early embryogenesis. The onset of Ac45LP mRNA expression at *Xenopus* embryonic stage-11 coincides with the first signs of neural crest induction [34]. Intriguingly, the withdrawal of neural crest from stage-25 spinal cords onwards [30] occurs concomitantly with the reduction in Ac45LP mRNA expression. The detection of both Ac45 and Ac45LP mRNA in migrating neural crest cells suggests a role for specialized V-ATPase functioning in these later developmental stages. For example, the V-ATPase may regulate the secretion of plasminogen activators that function in the breakdown of extracellular matrix tissue components during neural crest cell migration [35].

A remarkable finding of our study was the restricted expression of Ac45LP in only lung and kidney of *Xenopus*. Interestingly, both lung and kidney express specific V-ATPase subunit isoforms in specialized cell types [36]. In mammals, the lung epithelium contains two kinds of pneumonocytes, namely type I alveolar cells, which function in gas exchange, and type II alveolar cells, which express V-ATPase subunit isoforms in lamellar bodies that store and secrete surfactants and are thought to control the extracellular pH in the alveolus by active proton secretion [37]. The frog lung, however, contains only one type of pneumonocyte that combines both alveolar type I and II functions [38, 39]. One possibility is that the two combined functions of the frog pneumonocyte are made possible due to the presence of both Ac45 and Ac45LP. With respect to the presence of Ac45LP in the *Xenopus* kidney, it is interesting to note that in amphibians the mesonephros is extended with additional posterior tubules and forms the opisthonephros as the functional kidney; in contrast, the mammalian adult functional kidney develops from the metanephros [40]. It remains to be established whether the availability of the Ac45LP underlies this difference in the origin of the mammalian and frog kidney.

Of evolutionary interest is the absence of Ac45LP in not only mammals but also fish. It would appear that not only the mammalian lung and kidney can function without Ac45LP but also gills, which in fish represent the equivalent of the mammalian pulmonary and renal cells [41]. Thus, these two evolutionarily clearly separated groups of animals apparently function in the absence of Ac45LP.

In conclusion, we identified the first isoform of a V-ATPase accessory subunit and determined that this novel

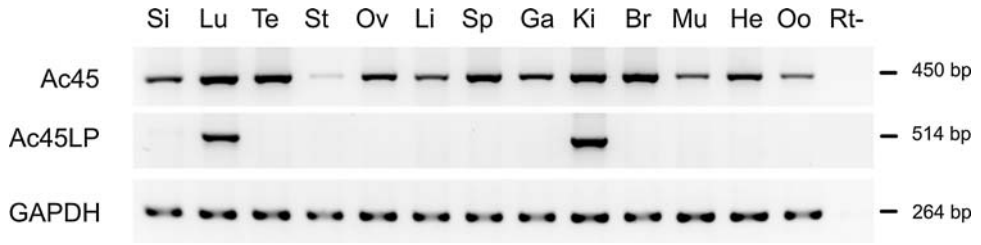

Fig. 7 Tissue distributions of *Xenopus* Ac45 and Ac45LP mRNAs. RNA was extracted from various tissues and RT-PCR analysis was performed as described in the Material and Methods. GAPDH served as an internal control for RNA integrity. *Si* Small intestine, *Lu* lung, *Te* testes, *St* stomach, *Ov* ovary, *Li* liver, *Sp* spleen, *Ga* gall bladder, *Ki* kidney, *Br* brain, *Mu* muscle, *He* heart, *Oo* oocytes, *Rt* absence of reverse transcriptase (negative control)

protein shares biochemical characteristics with Ac45, with the exception of its post-translational proteolytic processing and its expression pattern both during development and in the adult. The Ac45LP represents an Ac45 paralog that probably arose from an ancestral Ac45 gene duplication event, and the duplicated gene was sustained in tetrapod species. However, in placental mammals, the Ac45LP gene was lost. We conclude that in non-mammalian tetrapods, not only 'common' V-ATPase subunit isoforms but also an isoform of the accessory subunit Ac45 may contribute to yet another level of V-ATPase regulation during neurodevelopment and in specialized cells.

Acknowledgments The authors thank Dr. François van Herp (Radboud University Nijmegen) for helpful discussions, Anne Sinke and Emmy Zeetsen for technical assistance, and Ron Engels for animal care.

References

1. Adams DS, Robinson KR, Fukumoto T, Yuan S, Albertson RC, Yelick P, Kuo L, McSweeney M, Levin M (2006) Early, H^+V-ATPase-dependent proton flux is necessary for consistent left-right patterning of non-mammalian vertebrates. Development 133:1657–1671
2. Nishi T, Forgac M (2002) The vacuolar (H^+)-ATPases—nature's most versatile proton pumps. Nat Rev Mol Cell Biol 3:94–103
3. Paroutis P, Touret N, Grinstein S (2004) The pH of the secretory pathway: measurement, determinants, and regulation. Physiology (Bethesda) 19:207–215
4. Schoonderwoert VT, Martens GJ (2001) Proton pumping in the secretory pathway. J Membr Biol 182:159–169
5. Wagner CA, Finberg KE, Breton S, Marshansky V, Brown D, Geibel JP (2004) Renal vacuolar H^+-ATPase. Physiol Rev 84:1263–1314
6. Xu J, Cheng T, Feng HT, Pavlos NJ, Zheng MH (2007) Structure and function of V-ATPases in osteoclasts: potential therapeutic targets for the treatment of osteolysis. Histol Histopathol 22:443–454
7. Schoonderwoert VT, Martens GJ (2002) Targeted disruption of the mouse gene encoding the V-ATPase accessory subunit Ac45. Mol Membr Biol 19:67–71
8. Inoue H, Noumi T, Nagata M, Murakami H, Kanazawa H (1999) Targeted disruption of the gene encoding the proteolipid subunit of mouse vacuolar H^+-ATPase leads to early embryonic lethality. Biochim Biophys Acta 1413:130–138
9. Allan AK, Du J, Davies SA, Dow JA (2005) Genome-wide survey of V-ATPase genes in Drosophila reveals a conserved renal phenotype for lethal alleles. Physiol Genomics 22:128–138
10. Nuckels RJ, Ng A, Darland T, Gross JM (2009) The vacuolar-ATPase complex regulates retinoblast proliferation and survival, photoreceptor morphogenesis, and pigmentation in the zebrafish eye. Invest Ophthalmol Vis Sci 50:893–905
11. Hinton A, Bond S, Forgac M (2009) V-ATPase functions in normal and disease processes. Pflugers Arch 457:589–598
12. Kawasaki-Nishi S, Yamaguchi A, Forgac M, Nishi T (2007) Tissue specific expression of the splice variants of the mouse vacuolar proton-translocating ATPase a4 subunit. Biochem Biophys Res Commun 364:1032–1036
13. Oka T, Murata Y, Namba M, Yoshimizu T, Toyomura T, Yamamoto A, Sun-Wada GH, Hamasaki N, Wada Y, Futai M (2001) a4, a unique kidney-specific isoform of mouse vacuolar H^+-ATPase subunit a. J Biol Chem 276:40050–40054
14. Smith AN, Finberg KE, Wagner CA, Lifton RP, Devonald MA, Su Y, Karet FE (2001) Molecular cloning and characterization of Atp6n1b: a novel fourth murine vacuolar H^+-ATPase a-subunit gene. J Biol Chem 276:42382–42388
15. Brown D, Hirsch S, Gluck S (1988) An H^+-ATPase in opposite plasma membrane domains in kidney epithelial cell subpopulations. Nature 331:622–624
16. Smith AN, Borthwick KJ, Karet FE (2002) Molecular cloning and characterization of novel tissue-specific isoforms of the human vacuolar H^+-ATPase C, G and d subunits, and their evaluation in autosomal recessive distal renal tubular acidosis. Gene 297:169–177
17. Sun-Wada GH, Tabata H, Kawamura N (2005) Selective assembly of V-ATPase subunit isoforms in mouse kidney. J Bioenerg Biomembr 37:415–418
18. Poea-Guyon S, Amar M, Fossier P, Morel N (2006) Alternative splicing controls neuronal expression of v-ATPase subunit a1 and sorting to nerve terminals. J Biol Chem 281:17164–17172
19. Oka T, Toyomura T, Honjo K, Wada Y, Futai M (2001) Four subunit a isoforms of Caenorhabditis elegans vacuolar H^+-ATPase: cell-specific expression during development. J Biol Chem 276:33079–33085
20. Pietrement C, Sun-Wada GH, Silva ND, McKee M, Marshansky V, Brown D, Futai M, Breton S (2006) Distinct expression patterns of different subunit isoforms of the V-ATPase in the rat epididymis. Biol Reprod 74:185–194

21. Sun-Wada GH, Murata Y, Namba M, Yamamoto A, Wada Y, Futai M (2003) Mouse proton pump ATPase C subunit isoforms (C2-a and C2-b) specifically expressed in kidney and lung. J Biol Chem 278:44843–44851
22. Supek F, Supekova L, Mandiyan S, Pan YC, Nelson H, Nelson N (1994) A novel accessory subunit for vacuolar H(+)-ATPase from chromaffin granules. J Biol Chem 269:24102–24106
23. Getlawi F, Laslop A, Schagger H, Ludwig J, Haywood J, Apps D (1996) Chromaffin granule membrane glycoprotein IV is identical with Ac45, a membrane-integral subunit of the granule's H(+)-ATPase. Neurosci Lett 219:13–16
24. Holthuis JC, Jansen EJ, Schoonderwoert VT, Burbach JP, Martens GJ (1999) Biosynthesis of the vacuolar H^+-ATPase accessory subunit Ac45 in *Xenopus* pituitary. Eur J Biochem 262:484–491
25. Feng H, Cheng T, Pavlos NJ, Yip KH, Carrello A, Seeber R, Eidne K, Zheng MH, Xu J (2008) Cytoplasmic terminus of vacuolar type proton pump accessory subunit Ac45 is required for proper interaction with V(0) domain subunits and efficient osteoclastic bone resorption. J Biol Chem 283:13194–13204
26. Holthuis JC, Jansen EJ, van Riel MC, Martens GJ (1995) Molecular probing of the secretory pathway in peptide hormone-producing cells. J Cell Sci 108(Pt 10):3295–3305
27. Jansen EJ, Scheenen WJ, Hafmans TG, Martens GJ (2008) Accessory subunit Ac45 controls the V-ATPase in the regulated secretory pathway. Biochim Biophys Acta 1783:2301–2310
28. Waterhouse AM, Procter JB, Martin DM, Clamp M, Barton GJ (2009) Jalview Version 2–a multiple sequence alignment editor and analysis workbench. Bioinformatics 25:1189–1191
29. Chevenet F, Brun C, Banuls AL, Jacq B, Christen R (2006) TreeDyn: towards dynamic graphics and annotations for analyses of trees. BMC Bioinformatics 7:439
30. Nieuwkoop P, Faber J (1967) Normal table of *Xenopus laevis* (Daudin), 2nd edn. North Holland Publ, Amsterdam
31. Schoonderwoert VT, Martens GJ (2002) Structural gene organization and evolutionary aspects of the V-ATPase accessory subunit Ac45. Biochim Biophys Acta 1574:245–254
32. Louagie E, Taylor NA, Flamez D, Roebroek AJ, Bright NA, Meulemans S, Quintens R, Herrera PL, Schuit F, Van de Ven WJ, Creemers JW (2008) Role of furin in granular acidification in the endocrine pancreas: identification of the V-ATPase subunit Ac45 as a candidate substrate. Proc Natl Acad Sci USA 105:12319–12324
33. Jansen EJ, Holthuis JC, McGrouther C, Burbach JP, Martens GJ (1998) Intracellular trafficking of the vacuolar H^+-ATPase accessory subunit Ac45. J Cell Sci 111(Pt 20):2999–3006
34. Mayor R, Morgan R, Sargent MG (1995) Induction of the prospective neural crest of *Xenopus*. Development 121:767–777
35. Menoud PA, Debrot S, Schowing J (1989) Mouse neural crest cells secrete both urokinase-type and tissue-type plasminogen activators in vitro. Development 106:685–690
36. Jefferies KC, Cipriano DJ, Forgac M (2008) Function, structure and regulation of the vacuolar (H^+)-ATPases. Arch Biochem Biophys 476:33–42
37. Lubman RL, Danto SI, Crandall ED (1989) Evidence for active H^+ secretion by rat alveolar epithelial cells. Am J Physiol 257:L438–L445
38. Meban C (1973) The pneumonocytes in the lung of *Xenopus laevis*. J Anat 114:235–244
39. Berezin A, da Silva Sasso W (1974) Electron microscopy of the pulmonary alveolar cells (granular pneumocytes) of normal and vagotomized amphibian (*Bufo icterus icterus*). Experientia 30:1074–1076
40. Kardong K (2002) Vertebrates: comparative anatomy, function, evolution. McGraw-Hill, New York
41. Evans DH, Piermarini PM, Choe KP (2005) The multifunctional fish gill: dominant site of gas exchange, osmoregulation, acid-base regulation, and excretion of nitrogenous waste. Physiol Rev 85:97–177